A Failsafe for Sensing Chromatid Tension in Mitosis with the Histone H3 Tail in *Saccharomyces cerevisiae*

Christopher J. Buehl,* Xiexiong Deng,† Jianjun Luo,†,1 Visarut Buranasudja,‡ Tony Hazbun,‡,§ and Min-Hao Kuo*,†,2

*Cell and Molecular Biology Program and †Department of Biochemistry and Molecular Biology, Michigan State University, East Lansing, Michigan 48824 and ‡Department of Medicinal Chemistry and Molecular Pharmacology and §Purdue University Center for Cancer Research, Purdue University, West Lafayette, Indiana 47907

ABSTRACT Mitotic fidelity is ensured by achieving biorientation on all paired chromosomes. The key signal for proper chromosome alignment is the tension between sister chromatids created by opposing poleward force from the spindles. In the budding yeast, the tension-sensing function requires that the Shugoshin protein, Shugoshin 1, be recruited to the centromeres and the neighboring pericentric regions. Concerted actions integrating proteins at centromeres and pericentromeres create highly specific Shugoshin 1 domains on mitotic chromosomes. We have previously reported that an important regulatory region on histone H3, termed the tension-sensing motif (TSM), is responsible for retaining Shugoshin 1 at pericentromeres. The TSM is negatively regulated by the acetyltransferase Gcn5p, but the underlying mechanism was elusive. In this work, we provide evidence that, when the TSM function is impaired, the histone H3 tail adopts a role that complements the damaged TSM to ensure faithful mitosis. This novel function of the H3 tail is controlled by Gcn5p, which targets selective lysine residues. Mutations to K14 and K23 ameliorate the mitotic defects resulting from TSM mutations. The restoration of faithful segregation is accompanied by regaining Shugoshin 1 access to the pericentric regions. Our data reveal a novel pathway for mitotic Shugoshin 1 recruitment and further reinforce the active role played by chromatins during their segregation in mitosis.

KEYWORDS Shugoshin 1; histone H3; spindle assembly checkpoint; Gcn5

A core functional and structural unit in eukaryotic chromatin is the nucleosome, which is composed of four canonical histone proteins (H2A, H2B, H3, and H4) and 147 bp of DNA (Luger *et al.* 1997). These histones not only provide a framework for packaging DNA within the nucleus, but also have important roles in a wide variety of cellular processes, including transcription (Zhang *et al.* 1998; Berger 2007), nuclear import (Blackwell *et al.* 2007), DNA replication (Ramachandran and Henikoff 2015), recombination (Hunt *et al.* 2013), and the cell cycle (Megee *et al.* 1995; Ng *et al.* 2013). Contrary to the general perception that chromosomes are merely passive cargos during cell division, work from our lab and others has demonstrated an active role for histones in mitotic control and maintaining chromosome fidelity during cell division (Luo *et al.* 2010, 2016; Yamagishi *et al.* 2010).

Eukaryotic cells ensure faithful segregation of sister chromatids through the action of the conserved Spindle Assembly Checkpoint (SAC). The SAC monitors both the attachment of spindle microtubules to the kinetochores as well as the existence of tension between sister chromatids held together by the cohesin complex (Lew and Burke 2003; Pinsky and Biggins 2005). Proper biorientation of chromosomes generates tension between sister chromatids due to the poleward pulling force by spindles. A family of proteins integral to the tension-sensing pathway of the SAC is the Shugoshin family. Shugoshins monitor the tension between sister chromatids and are well conserved throughout eukaryotes (Indjeian *et al.* 2005; Wang and Dai 2005; Kitajima *et al.* 2006; Yamagishi *et al.* 2008). Shugoshins are enriched at the centromeres and pericentric regions (Kitajima *et al.* 2005; Fernius and Hardwick 2007; Haase *et al.* 2012) from which the tension originates (Bloom *et al.* 2006). In *Schizosaccharomyces pombe*, Shugoshin

doi: https://doi.org/10.1534/genetics.117.300606
Manuscript received July 14, 2017; accepted for publication December 8, 2017; published Early Online December 12, 2017.
[1]Present address: Institute of Biophysics, Chinese Academy of Sciences, Beijing, China, 100101.
[2]Corresponding author: Department of Biochemistry and Molecular Biology, 401 Biochemistry Building, Michigan State University, East Lansing, MI 48824. E-mail: kuom@msu.edu

Table 1 Yeast strains used in this study

Strain	Relevant Genotype	Source or Reference
227a	*lys1*	Gift of E. Grayhack
70α	*thr3 met*$^-$	Gift of E. Grayhack
yCB006	*MATa ade2-1 can1-100 his3-11,15 leu2-3,112 trp1-1 ura3-1 hht1-hhf1::KAN hht2-hhf2::KAN hta1-htb1::Nat hta2-htb2::HPH pMK439 ΔN [ARS CEN LEU2 HTA1-HTB1 hht2-Δ2-28-HHF2]*	This study
yCB007	*MATa ade2-1 can1-100 his3-11,15 leu2-3,112 trp1-1 ura3-1 hht1-hhf1::KAN hht2-hhf2::KAN hta1-htb1::Nat hta2-htb2::HPH pMK439 ΔN G44S [ARS CEN LEU2 HTA1-HTB1 hht2-Δ2-28 G44S-HHF2]*	This study
yCB031	*MATa ade2-1 can1-100 his3-11,15 leu2-3,112 trp1-1 ura3-1 hht1-hhf1::KAN hht2-hhf2::KAN hta1-htb1::Nat hta2-htb2::HPH pMK439 4K-A [ARS CEN LEU2 HTA1-HTB1 hht2-K9A-K14A-K18A-K23A-HHF2]*	This study
yCB032	*MATa ade2-1 can1-100 his3-11,15 leu2-3,112 trp1-1 ura3-1 hht1-hhf1::KAN hht2-hhf2::KAN hta1-htb1::Nat hta2-htb2::HPH pMK439 4K-A G44S [ARS CEN LEU2 HTA1-HTB1 hht2-K9A-K14A-K18A-K23A-G44S-HHF2]*	This study
yCB033	*MATa ade2-1 can1-100 his3-11,15 leu2-3,112 trp1-1::sgo1::TRP1 ura3-1 hht1-hhf1::KAN hht2-hhf2::KAN hta1-htb1::Nat hta2-htb2::HPH pQQ18 [ARS CEN LEU2 HTA1-HTB1 HHT2-HHF2]*	This study
yCB034	*MATa ade2-1 can1-100 his3-11,15 leu2-3,112 trp1-1::sgo1::TRP1 ura3-1 hht1-hhf1::KAN hht2-hhf2::KAN hta1-htb1::Nat hta2-htb2::HPH pMK439 4K-A [ARS CEN LEU2 HTA1-HTB1 hht2-K9A-K14A-K18A-K23A-HHF2]*	This study
yCB035	*MATa ade2-1 can1-100 his3-11,15 leu2-3,112 trp1-1::sgo1::TRP1 ura3-1 hht1-hhf1::KAN hht2-hhf2::KAN hta1-htb1::Nat hta2-htb2::HPH pMK439 4K-A G44S [ARS CEN LEU2 HTA1-HTB1 hht2-K9A-K14A-K18A-K23A-G44S-HHF2]*	This study
yCB060	*MATa ade2-1 can1-100 his3-11,15 leu2-3,112 trp1-1 ura3-1 hht1-hhf1::KAN hht2-hhf2::KAN hta1-htb1::Nat hta2-htb2::HPH pMK439 K14A G44S [ARS CEN LEU2 HTA1-HTB1 hht2-K14A-G44S-HHF2]*	This study
yCB066	*MATa ade2-1 can1-100 his3-11,15 leu2-3,112 trp1-1 ura3-1 hht1-hhf1::KAN hht2-hhf2::KAN hta1-htb1::Nat hta2-htb2::HPH pMK439 K14A [ARS CEN LEU2 HTA1-HTB1 hht2-K14A-HHF2]*	This study
yCB068	*MATa ade2-1 can1-100 his3-11,15 leu2-3,112 trp1-1 ura3-1 hht1-hhf1::KAN hht2-hhf2::KAN hta1-htb1::Nat hta2-htb2::HPH pMK439 K9A [ARS CEN LEU2 HTA1-HTB1 hht2-K9A-HHF2]*	This study
yCB115	*MATa ade2-1 can1-100 his3-11,15 leu2-3,112 trp1-1 ura3-1 hht1-hhf1::KAN hht2-hhf2::KAN hta1-htb1::Nat hta2-htb2::HPH pMK439 K23A G44S [ARS CEN LEU2 HTA1-HTB1 hht2-K23A-G44S-HHF2]*	This study
yCB116	*MATa ade2-1 can1-100 his3-11,15 leu2-3,112 trp1-1 ura3-1 hht1-hhf1::KAN hht2-hhf2::KAN hta1-htb1::Nat hta2-htb2::HPH pMK439 K18A G44S [ARS CEN LEU2 HTA1-HTB1 hht2-K18A-G44S-HHF2]*	This study
yCB168	*MATa ade2-1 can1-100 his3-11,15 leu2-3,112 trp1-1 ura3-1 hht1-hhf1::KAN hht2-hhf2::KAN hta1-htb1::Nat hta2-htb2::HPH pMK439 K23A [ARS CEN LEU2 HTA1-HTB1 hht2-K23A-HHF2]*	This study
yCB203	*MATa ade2-1 can1-100 his3-11,15 leu2-3,112 trp1-1 ura3-1 hht1-hhf1::KAN hht2-hhf2::KAN hta1-htb1::Nat hta2-htb2::HPH pMK439 K18A [ARS CEN LEU2 HTA1-HTB1 hht2-K18A-HHF2]*	This study
yCB207	*MATa ade2-1 can1-100 his3-11,15 leu2-3,112 trp1-1 ura3-1 hht1-hhf1::KAN hht2-hhf2::KAN hta1-htb1::Nat hta2-htb2::HPH pMK439 4K-R G44S [ARS CEN LEU2 HTA1-HTB1 hht2-K9R-K14R-K18R-K23R-G44S-HHF2]*	This study
yCB208	*MATa ade2-1 can1-100 his3-11,15 leu2-3,112 trp1-1 ura3-1 hht1-hhf1::KAN hht2-hhf2::KAN hta1-htb1::Nat hta2-htb2::HPH pMK439 K9A G44S [ARS CEN LEU2 HTA1-HTB1 hht2-K9A-G44S-HHF2]*	This study
yCB233	*MATa ade2-1 can1-100 his3-11,15 leu2-3,112 trp1-1 ura3-1 hht1-hhf1::KAN hht2-hhf2::KAN hta1-htb1::Nat hta2-htb2::HPH pMK439 4K-R [ARS CEN LEU2 HTA1-HTB1 hht2-K9R-K14R-K18R-K23R-HHF2]*	This study
yCB317	*MATa/α his3Δ1 leu2Δ0 met15Δ0 ura3Δ0 hht1-hhf1::KAN hhf2-hht2::NAT hta1-htb1::HPH hta2-htb2::NAT pMK439 K14A [ARS CEN LEU2 HTA1-HTB1 hht2-K14A-HHF2]*	This study
yCB318	*MATa/α his3Δ1 leu2Δ0 met15Δ0 ura3Δ0 hht1-hhf1::KAN hhf2-hht2::NAT hta1-htb1::HPH hta2-htb2::NAT pMK439 K14A G44S [ARS CEN LEU2 HTA1-HTB1 hht2-K14A-G44S-HHF2]*	This study

(continued)

Table 1, *continued*

Strain	Relevant Genotype	Source or Reference
yCB325	*MATa ade2-1 can1-100 his3-11,15 leu2-3,112 trp1-1 ura3-1 hht1-hhf1::KAN hht2-hhf2::KAN hta1-htb1::Nat hta2-htb2::HPH pMK439 K14A T45A [ARS CEN LEU2 HTA1-HTB1 hht2-K14A-T45A-HHF2]*	This study
yCB326	*MATa ade2-1 can1-100 his3-11,15 leu2-3,112 trp1-1 ura3-1 hht1-hhf1::KAN hht2-hhf2::KAN hta1-htb1::Nat hta2-htb2::HPH pMK439 K14A K42A [ARS CEN LEU2 HTA1-HTB1 hht2-K14A-K42A-HHF2]*	This study
yCB343	*MATa ade2-1 bar1::URA3 can1-100 his3-11,15 leu2-3,112 trp1-1::SGO1-6xHA::TRP1 ura3-1 hht1-hhf1::KAN hht2-hhf2::KAN hta1-htb1::Nat hta2-htb2::HPH pMK439 K14A [ARS CEN LEU2 HTA1-HTB1 hht2-K14A-HHF2]*	This study
yCB344	*MATa ade2-1 bar1::URA3 can1-100 his3-11,15 leu2-3,112 trp1-1::SGO1-6xHA::TRP1 ura3-1 hht1-hhf1::KAN hht2-hhf2::KAN hta1-htb1::Nat hta2-htb2::HPH pMK439 K14A G44S [ARS CEN LEU2 HTA1-HTB1 hht2-K14A-G44S-HHF2]*	This study
yJL145	*MATa ade2-1 can1-100 his3-11,15 leu2-3,112 trp1-1 ura3-1 hht1-hhf1::KAN hht2-hhf2::KAN hta1-htb1::Nat hta2-htb2::HPH pMK439 G44S [ARS CEN LEU2 HTA1-HTB1 hht2-G44S-HHF2]*	Luo *et al.* (2010)
yJL170	*MATa ade2-1 can1-100 his3-11,15 leu2-3,112 trp1-1::sgo1::TRP1 ura3-1 hht1-hhf1::KAN hht2-hhf2::KAN hta1-htb1::Nat hta2-htb2::HPH pMK439 G44S [ARS CEN LEU2 HTA1-HTB1 hht2-G44S-HHF2]*	This study
yJL340	*MATa/α his3Δ1 leu2Δ0 met15Δ0 ura3Δ0 hht1-hhf1::KAN hhf2-hht2::NAT hta1-htb1::HPH hta2-htb2::NAT pMK439 G44S [ARS CEN LEU2 HTA1-HTB1 hht2-G44S-HHF2]*	Luo *et al.* (2016)
yJL467	*MATa ade2-1 can1-100 his3-11,15 leu2-3,112 trp1-1 ura3-1 hht1-hhf1::KAN hht2-hhf2::KAN hta1-htb1::Nat hta2-htb2::HPH pMK439 K42A [ARS CEN LEU2 HTA1-HTB1 hht2-K42A-HHF2]*	This study
yJL471	*MATa ade2-1 can1-100 his3-11,15 leu2-3,112 trp1-1 ura3-1 hht1-hhf1::KAN hht2-hhf2::KAN hta1-htb1::Nat hta2-htb2::HPH pMK439 T45A [ARS CEN LEU2 HTA1-HTB1 hht2-T45A-HHF2]*	This study
yMK1174	*MATa/α his3Δ1 leu2Δ0 met15Δ0 ura3Δ0 hht1-hhf1::KAN hhf2-hht2::NAT hta1-htb1::HPH hta2-htb2::NAT pJH33 [ARS CEN URA3 HTA1-HTB1 HHT2-HHF2]*	Luo *et al.* (2016)
yMK1243	*MATa ade2-1 can1-100 his3-11,15 leu2-3,112 trp1-1 ura3-1 hht1-hhf1::KAN hht2-hhf2::KAN hta1-htb1::Nat hta2-htb2::HPH pQQ18 [ARS CEN LEU2 HTA1-HTB1 HHT2-HHF2]*	Luo *et al.* (2010)
yXD143	*MATa ade2-1 bar1::URA3 can1-100 his3-11,15 leu2-3,112 trp1-1::SGO1-6xHA::TRP1 ura3-1 hht1-hhf1::KAN hht2-hhf2::KAN hta1-htb1::Nat hta2-htb2::HPH pQQ18 [ARS CEN LEU2 HTA1-HTB1 HHT2-HHF2]*	This study
yXD144	*MATa ade2-1 bar1::URA3 can1-100 his3-11,15 leu2-3,112 trp1-1::SGO1-6xHA::TRP1 ura3-1 hht1-hhf1::KAN hht2-hhf2::KAN hta1-htb1::Nat hta2-htb2::HPH pMK439 G44S [ARS CEN LEU2 HTA1-HTB1 hht2-G44S-HHF2]*	This study

1 (Sgo1) is recruited to these regions by binding directly to histone H2A, which is phosphorylated by the Bub1 kinase, as well as to specific heterochromatin marks on histones (Kawashima *et al.* 2010; Yamagishi *et al.* 2010). The budding yeast *Saccharomyces cerevisiae* lacks these heterochromatin marks, and therefore the centromeric Bub1p-mediated histone H2A S121 phosphorylation provides the major nucleation for the recruitment of Sgo1p (Fernius and Hardwick 2007; Kawashima *et al.* 2010). We have reported that the tension-sensing motif (TSM), ^{42}KPGT, of histone H3 is critical to the pericentric recruitment of Sgo1p (Luo *et al.* 2010, 2016). Point mutations within this motif diminish pericentric Sgo1p recruitment without significantly affecting its centromeric localization. Mitotic phenotypes that result from these TSM mutations include chromosomal instability and missegregation, and the inability to activate the SAC when there is no tension between sister chromatids. These phenotypes overlap with those seen with *SGO1* deletion, and can be rescued by overexpressing or by artificially tethering Sgo1p to the pericentric chromatin, suggesting that maintaining Sgo1p at or near the centromeres feeds the tension status signal to the SAC.

Recently, we showed that Sgo1p pericentric recruitment is regulated by the histone acetyltransferase Gcn5p (Luo *et al.* 2016). Deleting *GCN5* or overexpressing a catalytically inactive form of Gcn5p rescues *tsm*$^-$ mitotic defects. Deleting a histone deacetylase, *RPD3*, enhances the chromosomal instability defect. These data suggest a role for acetylation in the tension-sensing function of the SAC. Lysine residues in the histone H3 tail, most prominently K14, are well-characterized targets of Gcn5p acetyltransferase activity (Kuo *et al.* 1996). Indeed, a role of Gcn5p and H3 acetylation in centromeric function has been reported (Vernarecci *et al.* 2008). In this report, we demonstrate that in a *tsm*$^-$ background, cells require the histone H3 tail to survive when put under mitotic stress. The mitotic defects of *tsm*$^-$ mutants can be alleviated by replacing the H3 tail lysine residues with alanine, specifically

Table 2 Plasmid constructs used in this study

Plasmid	Main Features	Source or Reference
pCB034	pGEX-4T-1 *3xHA-SUMO*	This study
pCB035	pGEX-4T-1 *3xHA-SUMO-SGO1*	This study
pCB043	pGEX-6P-1 *GST-[2-135 CSE4]*	This study
pCB044	pGEX-6P-1 *GST-[2-150 CNN1]*	This study
pCB045	pGEX-6P-1 *GST-[2-38 HHT2]*	This study
pJH33/pMK439	pRS316-*HTA1-HTB1 HHT2-HHF2*	Luo *et al.* (2010)
pMK120	2 μm *URA3* vector with *CUP1* promoter	Kuo *et al.* (1998)
pMK144	2 μm *URA3 pCUP1-GCN5*	Kuo *et al.* (1998)
pMK144 E173H	2 μm *URA3 pCUP1-gcn5E173H*	Kuo *et al.* (1998)
pMK515	pET21 *6xHis-GCN5*	Liu *et al.* (2005)
pYCF1/CEN3.L	YRp14/TEL cassette (pYCF1) with a *CEN3* insert	Spencer *et al.* (1990)

K14. Sgo1p binds the histone H3 tail, allowing the H3 tail to act as a secondary site of Sgo1p binding to ensure SAC function when the TSM is crippled.

Materials and Methods

Yeast strains and plasmid constructs

The yeast strains, plasmids, and oligos used in this work are listed in Table 1, Table 2, and Table 3, respectively.

Histone mutations were generated in pMK439 by two-step PCR site-directed mutagenesis (Luo *et al.* 2010). Yeast transformations were performed by the lithium acetate method (Gietz *et al.* 1992). 5-FOA selection was conducted to select for yeast cells that had lost the plasmid pMK440 (a *URA3* plasmid bearing all four core histone genes).

Yeast methods

Yeast growth media, conditions, and transformations were based on standard procedures (Sherman 1991). When appropriate, 5% casamino acids (CAA) were used to substitute for synthetic amino acid mixtures as selective medium for uracil, tryptophan, or adenine prototrophs.

Spot assays were performed with logarithmically growing cultures, which were diluted to 0.1 OD_{600}/ml in 100 μl sterile H_2O. Three 1:10 serial dilutions into 100 μl sterile H_2O were subsequently prepared, and 5 μl of each dilution were spotted onto YPD plates containing 0, 5, 7.5, or 10 μg/ml benomyl and grown at 30° for 2 days before analysis.

Mating assays to assess chromosome stability were conducted by patching diploid cells from single colonies to YPD plates and incubated at 30° for 2–3 days until saturation. Cell patches were replica-plated YPD plates prespread with a or α tester cells (227a or 70α, respectively) and allowed to mate at 30° before replica plating again to synthetic minimal medium. Mating between the tester and the subject strains resulted in complete complementation of nutrient requirement and hence colonies on the minimal medium. The number of colonies that grew from each patch was counted and used to assess the relative rate for chromosome loss.

Western analyses of yeast proteins were conducted as described in reference (Luo *et al.* 2010).

Red sectoring assays were performed as described by Spencer *et al.* (1990). Briefly, strains were transformed with plasmid pYCF1/CEN3.L linearized with *Bgl*II. Ura^+ transformants were grown in CAA-Ura medium overnight and then plated directly onto YPD plates for colony formation and scoring.

Chromatin immunoprecipitation (ChIP)

Yeast cultures for ChIP were grown in YPD to log phase and arrested with 2 μg/ml α factor for 4 hr in a 30° shaker, pelleted, and washed with sterile water. Cell pellets were resuspended in the original volume of YPD, and allowed to grow for 60 min at 30° before cells were cross-linked with 1% formaldehyde at room temperature for 45 min, washed with ice-cold Tris-buffered saline, and stored at −80°. ChIP was conducted as previously described (Kuo *et al.* 1998; Luo *et al.* 2010). ChIP results were quantified using quantitative PCR performed on a Roche LightCycler 480 and normalized with 0.1% inputs.

Fluorescence-activated cell sorting (FACS)

Yeast cultures were grown in YPD to log phase and arrested with 200 μM hydroxyurea (HU) for 3 hr in a 30° shaker, pelleted, and washed with sterile water. Cells were then released into fresh YPD, collected at various time points, and fixed with 70% ethanol for 45–90 min. Cells were rehydrated with PBS pH 7.4 at room temperature for 2 hr before

Table 3 Oligos used in this study

Oligo	Sequence
oCB007	AGGTCGAACATTTCTCACCA
oCB008	AGCCGTCCGATATATCCTCT
oCB023	CGAGAAGTAGTTCAAATGCAGA
oCB024	TGAGGACAGCCTATGGACATT
oCB031	CAACCACGCAATGAGTCTT
oCB032	TGGGGATATCTCAGAATGGA
oCB053	CCTCACGCGCTCTAATCC
oCB054	AGGAAGAAGACCCCAACGA
oCB123	CCCATCCGATACGAGCAT
oCB124	GGGAAGCCTGTGCGAAAT
oXD070	GCATAAGTGTGCCTTAGTATG
oXD071	GCGCTTGAAATGAAAGCTCCG

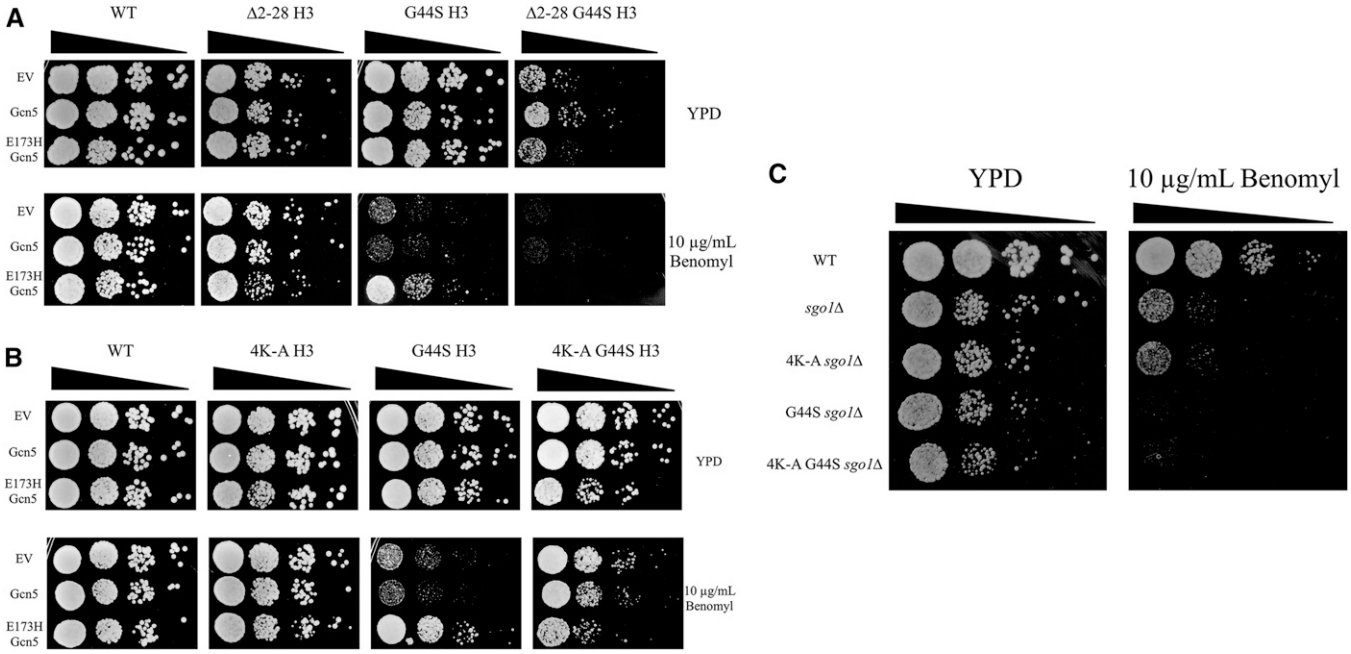

Figure 1 Tension-sensing motif (TSM) function is modulated by lysine residues within the histone H3 tail domain in an *SGO1*-dependent manner. (A) Strains with the listed histone H3 alleles were transformed with empty vector (EV) or overexpression plasmids for either wild-type (WT) or a catalytically inactive *E173H* Gcn5p. Logarithmically growing cultures were serially diluted and spotted to YPD or YPD containing 10 μg/ml benomyl. (B) Strains with histone H3 K9, 14, 18, and 23 mutated to alanine (4K-A) along with a WT or G44S TSM allele were assessed by spot assay as described above. (C) The 4K-A mutations were tested in Δ*sgo1* strains to assess the *SGO1* dependence of the 4K-A rescue.

overnight treatment at 37° with 100 μg/ml RNase A in 10 mM NaCl/50 mM Tris pH 7.4. Cells were pelleted, resuspended in PBS pH 7.4, and a final concentration of 40 μg/ml of propidium iodide was added to the cell suspension before FACS analysis with a BD LSR II flow cytometer.

Recombinant protein preparation

To express and purify 6His-SUMO-Sgo1p and 6His-Gcn5p from *Escherichia coli*, 100 ml BL21-CodonPlus *E. coli* cells were induced (at optical density 0.5–0.6 in LB with 50 μg/ml Kanamycin) with 1 mM IPTG at 16° for 16 hr. Cells were pelleted (5000 × *g* for 5 min at 4°) and resuspended in 10 ml Lysis/Sonication Buffer (300 mM NaCl, 50 mM Na_2HPO_4, 1 mM DTT, 1 mM PMSF, and 1 mg/ml lysozyme) and incubated on ice for 30 min. Cells were flash frozen and thawed twice. Cells were then sonicated six times, via 15-sec bursts, with 1 min on ice in between rounds of sonication. Debris was pelleted at 10,000 rpm for 15 min at 4°, and the soluble fraction was transferred to a new tube and mixed with 5 ml Ni-nitrilotriacetic acid (NTA) beads for purification of 6His tag. Beads were incubated at 4° for 1 hr, washed twice with 10 ml wash buffer (300 mM NaCl, 50 mM Na_2HPO_4, 1 mM DTT, 1 mM PMSF, and 10% glycerol) at pH 6.0, and once with 10 ml wash buffer at pH 5.5. 6His-SUMO was eluted with 6 ml wash buffer at pH 4.0 supplemented with 200 mM imidazole. The pH of the eluate was neutralized with 300 μl 1 M Na_2HPO_4. Purification of H3(2-38)-GST protein was the same, except the soluble fraction was mixed with 200 μl glutathione Sepharose beads, and washed three times with IPP-150 (10 mM Tris pH 8.0, 150 mM NaCl, 0.1% NP-40, 1 mM DTT, and 1 mM PMSF), and eluted with IPP-150 supplemented with 15 mM reduced glutathione at 4° for 1 hr. All protein yields and purities were assessed by SDS-PAGE analysis.

GST pulldown assay

H3(2-38)-GST was acetylated in reaction buffer (50 mM Tris pH 7.4, 50 mM NaCl, and 500 μM Acetyl CoA) by recombinant 6His-Gcn5p for 1 hr at 30°. Mock treatment was the same except lacking Acetyl CoA. H3(2-38)-GST, Ac H3(2-38)-GST, or GST was bound to glutathione Sepharose beads in IPP-150 for 1 hr at 4°. Beads were then mixed with equivalent moles of 6His-SUMO-Sgo1p or 6His-SUMO and incubated for 2 hr at 4°. Beads were washed four times with IPP-150, and retained proteins were eluted by boiling with SDS-PAGE loading dye and analyzed by western blot.

Data availability

All strains and plasmid constructs are available on request.

Results

The histone H3 tail provides a site for Gcn5p acetylation and mediates suppression of *tsm*$^-$ mitotic defects. Our previous results revealed a negative regulatory function of Gcn5p for the H3 TSM, in that the loss of Gcn5p or its HAT activity rescues the impaired SAC function (Luo *et al.* 2016). The converse effects can be seen with the deletion of *RPD3*, consistent with the opposing enzymatic activity of Rpd3p HDAC.

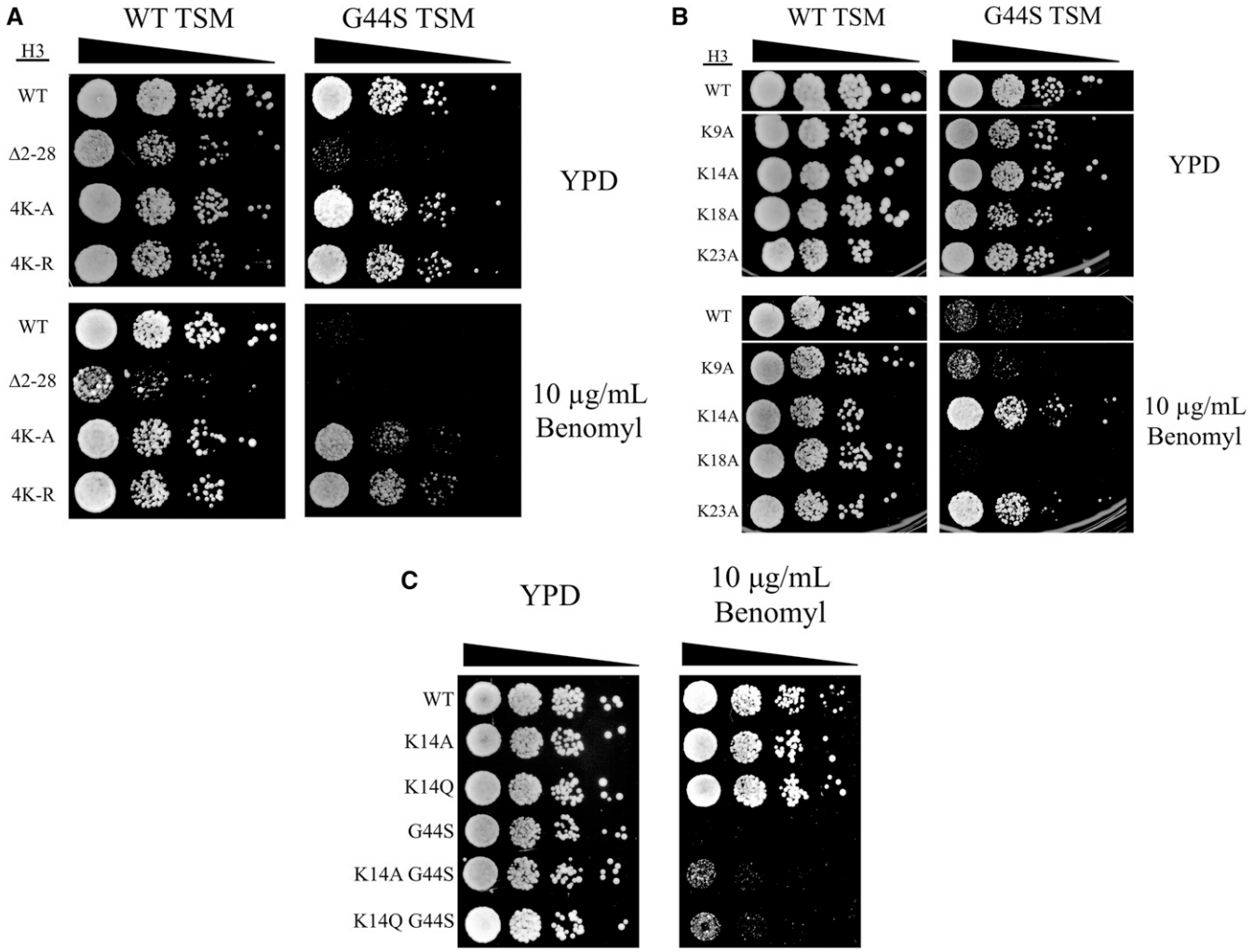

Figure 2 Single alanine or glutamine mutation of K14 rescues *tsm*$^-$ defects. Strains with the indicated H3 mutations were analyzed by spot assays. The effects of 4K-R (A), single alanine substitutions (B), and a K14Q mutation (C) on G44S benomyl hypersensitivity were assessed. TSM, tension-sensing motif; WT, wild-type.

Because Gcn5p and Rpd3p act on the H3 tail, we hypothesized that in *tsm*$^-$ strains, acetylation of the histone H3 tail or one of the downstream effectors of acetylation assumes a more pronounced mitotic role when the TSM function is crippled. To test this notion, we first removed the H3 tail by deleting residues 2–28. We also overexpressed wild-type Gcn5p or a catalytically dead allele, *gcn5-E173H*, to examine the involvement of the H3 tail in the TSM's function (Figure 1A). Deleting the H3 tail did not cause significant mitotic phenotypes, but when combined with the G44S *tsm*$^-$ allele, cells were sick without any stress. The role of the H3 tail in mitotic tension sensing was tested by cellular response to benomyl, a microtubule-destabilizing drug that exacerbates defects in tension sensing (Kawashima *et al.* 2011; Haase *et al.* 2012; Luo *et al.* 2016). As shown before (Luo *et al.* 2016), overexpressing *gcn5-E173H* rescues the benomyl hypersensitivity phenotype caused by the G44S *tsm*$^-$ mutation. However, this rescue was eradicated by the Δ2-28 H3 mutant, suggesting that the H3 tail is targeted by Gcn5p to regulate the function of the TSM. Because the tail deletion itself does not affect benomyl tolerance (see Δ2-28 H3 row 4), we suggest that the H3 tail is a TSM "sidekick" whose function becomes more appreciable when the TSM is crippled.

As H3 tail deletion causes G44S cells to become sick (see Δ2-28 G44S H3, row 1), a more targeted approach was taken. Lysine-to-alanine substitutions were made at residues 9, 14, 18, and 23 (4K-A). K14 is the primary site of Gcn5p acetylation, whereas K18 and K23 are secondary targets, and K9 is the least-efficient substrate for Gcn5p (Kuo *et al.* 1996; Zhang *et al.* 1998). Replacing these four lysine residues with alanine did not cause discernible phenotypes under normal growth conditions, with or without the G44S mutation (Figure 1B). Strikingly, the 4K-A allele alone was sufficient to rescue the G44S benomyl hypersensitivity phenotype (see 4K-A G44S, row 4). This allele does not add additional strength to the *gcn5-E173H* suppressor (see 4K-A G44S, row 6), suggesting a common mechanism of these two suppressors. To further verify the specificity of the 4K-A suppressor, we deleted *SGO1*, the

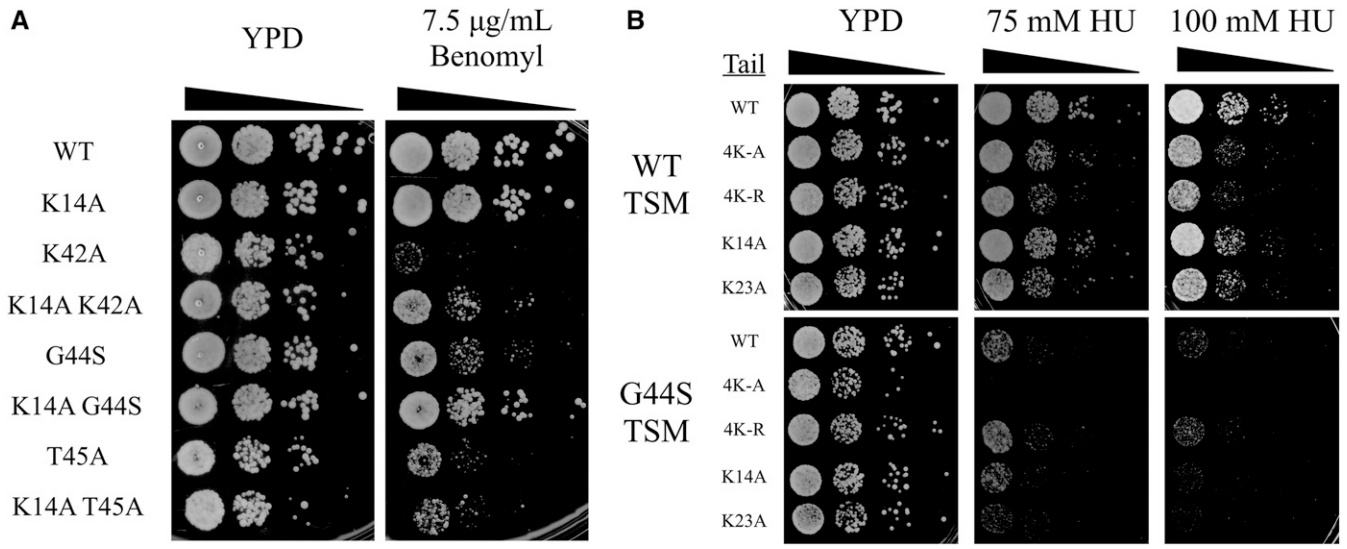

Figure 3 K14A rescues hypersensitivity of *tsm*$^{-}$ mutants to benomyl but not HU. HU, hydroxyurea; TSM, tension-sensing motif; WT, wild-type K14A was assessed buy spot assay for its ability to rescue benomyl hypersensitivity of other TSM mutations (A) and hypersensitivity to HU (B).

primary effector for TSM. When *SGO1* is deleted, the 4K-A allele no longer rescues the benomyl hypersensitivity of G44S (Figure 1C). Thus, Gcn5p most likely targets the lysine residues in the N' tail of histone H3 to regulate the function of the TSM.

Alanine substitution for lysine imposes a profoundly different structure from the original lysine side chain. To test if the 4K-A suppression of benomyl hypersensitivity was reliant on the loss of a positive charge, we tested 4K-R quadruple mutations to mimic the unacetylated lysine. The 4K-R allele provided a more robust rescue of G44S benomyl hypersensitivity than the 4K-A, perhaps due to the greater similarity of arginine to lysine than alanine (Figure 2A). Together, these results suggest that lysine *per se* is critical for the functional interaction between the tail and the TSM.

All lysine residues in the H3 tail are not acetylated with equal affinity by Gcn5p. The most preferred target of Gcn5p acetylation is K14, while K18 and K23 have also been identified as sites of Gcn5p-mediated acetylation (Kuo *et al.* 1996; Kuo and Andrews 2012). Therefore, we tested if mutations of any single lysine residue to alanine would be sufficient to rescue the G44S benomyl hypersensitivity (Figure 2B). The relative power of suppression in general correlated with the Gcn5p target preference: K14A rescued the G44S *tsm*$^{-}$ benomyl hypersensitivity very effectively. K23A displayed modest suppression, whereas K9A and K18A did not affect the G44S mitotic defect. While these results are consistent with the model that Gcn5p acetylation of the histone H3 tail lysine acts as a negative regulator for the TSM, the K14Q acetylation-mimicking mutation caused rescue comparable to that by the

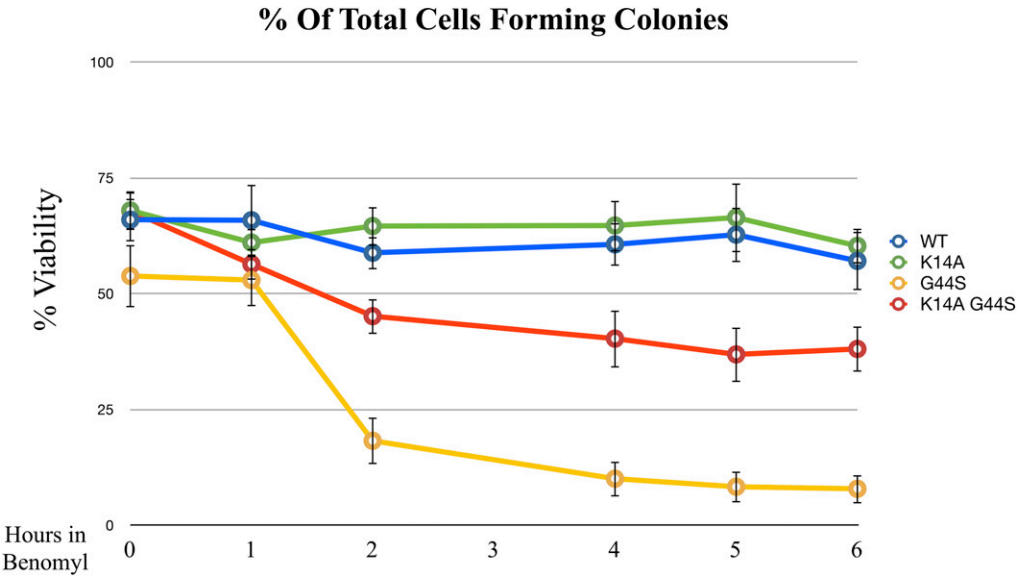

Figure 4 K14A mutation partially rescues recovery from benomyl arrest. Exponentially growing cells with the indicated histone H3 mutations were treated with 40 µg/ml benomyl for the indicated time. Colony forming units, expressed as % viability, were measured on benomyl-free YPD plates. Data are from three independent biological replicates, with the error bars representing the SD. WT, wild-type.

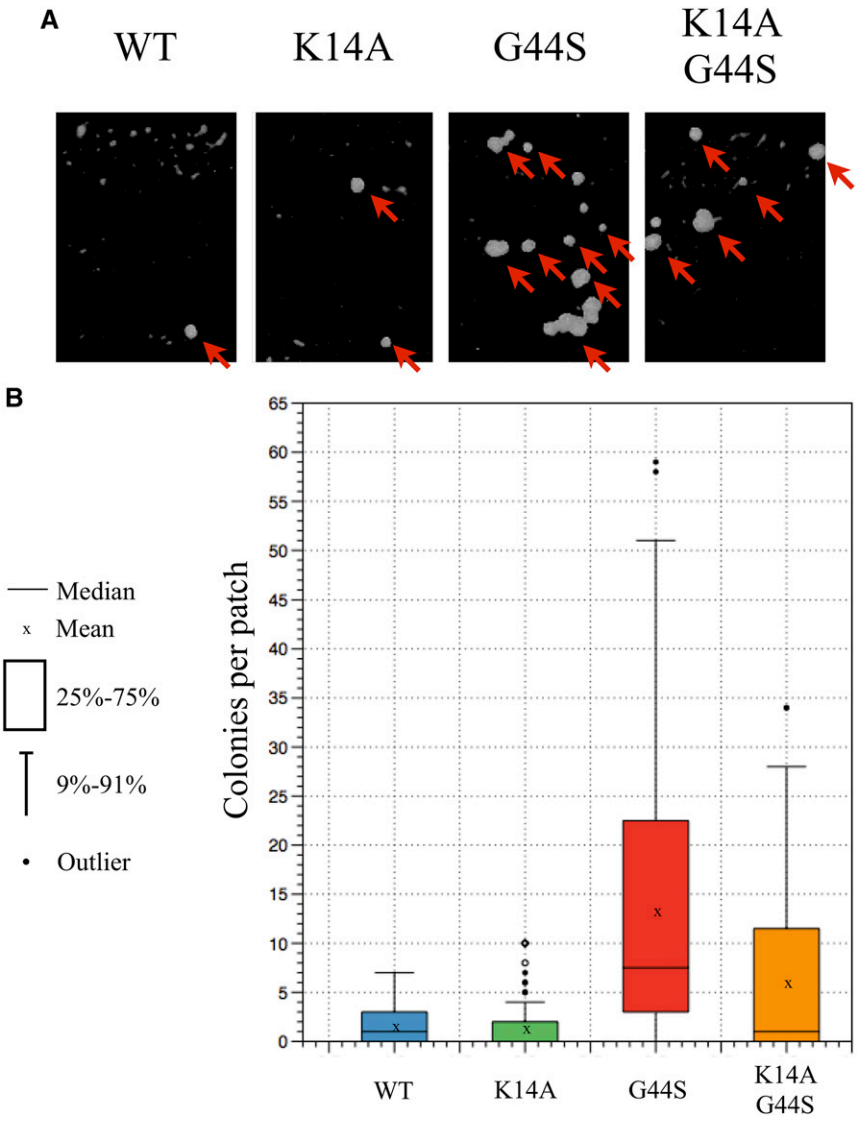

Figure 5 K14A rescues aberrant mating phenotypes of diploid *tsm*⁻ strain. Diploid strains containing the wild-type (WT), K14A, G44S, and K14A G44S alleles as the sole copy of H3 were subjected to mating with haploid tester strains. Colony formation on minimal medium indicates aberrant mating resulting from aneuploidy. (A) Representative images of colonies on minimal medium plates. Arrows indicate colony growth. (B) Colony growth shown by box plot. Data represents three independent biological replicates, and a total of 120 patches of each strain analyzed. Both WT and K14A strains show low levels of mating, which are greatly increased in the G44S strain. This aberrant mating can be reduced with the introduction of K14A into the G44S strain.

K14A mutation (Figure 2C). Though eliminating the positive charge of the lysine side chain, the structural differences between glutamine and acetylated lysine, as noted by Kasten *et al.* (2004), may have contributed to the suppression by crippling the normal Gcn5p-K14 acetylation regulation circuitry.

K14A suppresses the mitotic defects of different *tsm*⁻ mutants. The TSM consists of K42, P43, G44, and T45 (Luo *et al.* 2016), with alanine substitutions of any one residue except P43 resulting in mitotic defects. To gain a deeper understanding of the functional interaction between H3 K14 and the TSM, we also tested the suppressing activity of K14A in K42A and T45A *tsm*⁻ mutants. K14A demonstrated a strong rescue of K42A benomyl hypersensitivity (Figure 3A), and a modest rescue of T45A (data not shown). T45A causes the most severe phenotype among all TSM mutants (Luo *et al.* 2016), possibly due to the prevention of T45 phosphorylation, which is critical for DNA replication (Dai *et al.* 2008; Baker *et al.* 2010; Kawashima *et al.* 2011). The partial rescue of T45A may thus be attributed to the pleiotropic damages caused by this mutation. Consistent with this suggestion are the observations that hypersensitivities to HU and UV are also associated with mutations of the TSM (Luo *et al.* 2010, 2016). HU inhibits ribonucleotide reductase for deoxyribonucleotide synthesis during DNA replication (Slater 1973; Koc *et al.* 2004). HU hypersensitivity therefore likely indicates defects in DNA synthesis that are reminiscent of the additional role of T45 phosphorylation in the S phase. Importantly, this phenotype of *tsm*⁻ mutations is refractory to suppressors such as Sgo1p overexpression or *gcn5*Δ (Luo *et al.* 2010, 2016). To see whether H3 tail lysine mutations act selectively on the mitotic function of the TSM, cell growth in the presence of HU was tested (Figure 3B). None of the above tail mutations reduced the sensitivity to HU caused by the G44S *tsm*⁻ mutation, strongly suggesting that the tail domain of H3, the acetylatable lysine residues in particular, genetically interacts with the TSM for mitotic regulation.

Benomyl treatment is an efficient method to interrogate the SAC response, as it perturbs microtubule formation and consequently activates the SAC for the lack of both tension and

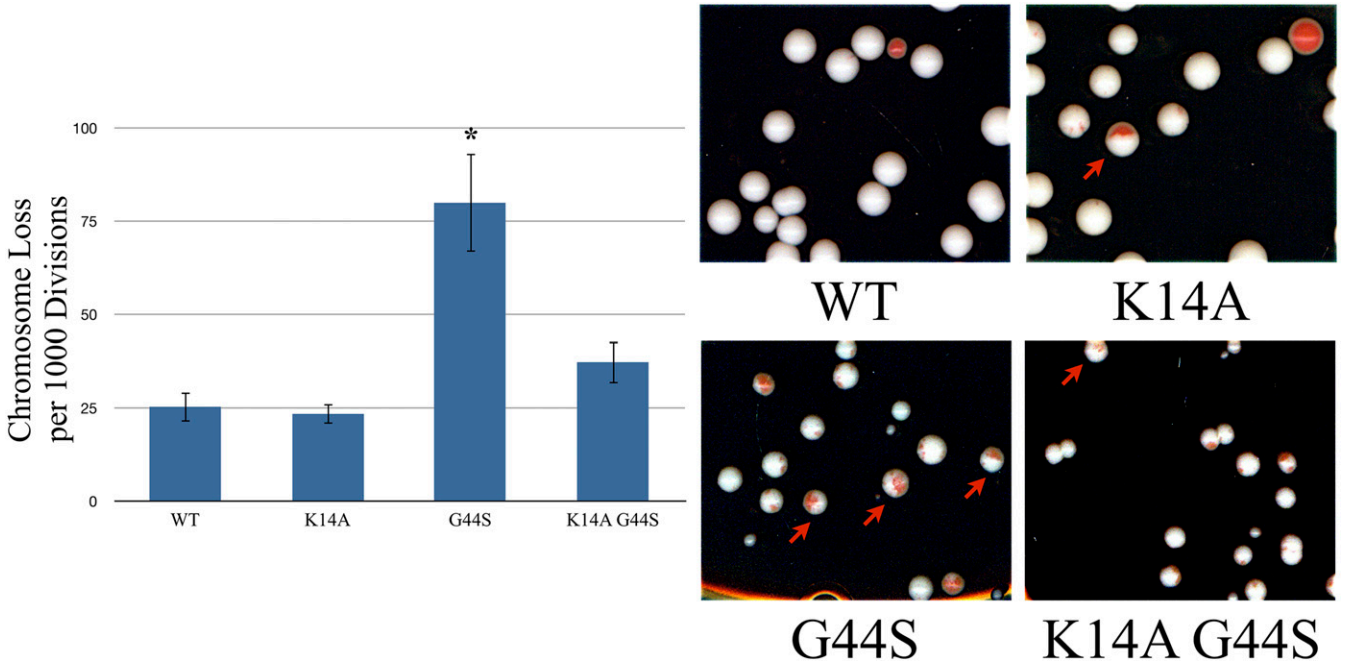

Figure 6 K14A restores chromosome stability of G44S *tsm*$^-$ cells. Strains with the indicated histone H3 backgrounds were transformed with a synthetic chromosome containing the *SUP11* gene that suppressed the ochre mutation of *ade2-1*. Loss of this synthetic chromosome is indicated by red sectoring in colonies. Half-red/half-white colonies were counted, as they indicated first-division chromosome loss. The left panel presents the quantification of chromosome loss per 1000 cells divisions as assayed by the method from three independent biological replicates of at least 150 colonies per replicate. Error bars represent SD. * indicates significantly different ($P < 0.05$) from wild-type, as assessed by Student's *t*-test.

spindle–kinetochore attachment. One additional approach to examining benomyl-induced tension defects is to treat cells with high doses of benomyl for a short period of time before plating cells to a benomyl-free culture plate. During the recovery phase, in which the spindle–kinetochore association is being reestablished, cells tend to commit erroneous attachment, leading to tensionless mistakes (Glotzer 1996; Loncarek *et al.* 2007). Elevated mortality indicates defects in tension sensing (Jeganathan *et al.* 2007; Santaguida and Amon 2015). To further link K14A and G44S mutations to the tension-sensing function, wild-type, K14A, G44S, and K14A G44S strains were first arrested by benomyl (40 μg/ml) for increasing time intervals, then washed and plated on YPD. As expected, both wild-type and K14A strains displayed minimal sensitivity to any length of benomyl treatment (Figure 4). The G44S *tsm*$^-$ strain showed rapid loss of viability after benomyl treatment. This phenotype was partially rescued by the K14A mutation, indicating that cells regained the ability to detect and to respond to defects in tension surveillance.

Improper segregation of sister chromatids results in chromosome instability and hence aneuploidy. To evaluate genome integrity, we exploited the mating systems of budding yeast. Haploid yeast possess one copy of either the *MAT***a** or *MAT*α mating locus on chromosome III. *MAT***a** cells are capable of mating with *MAT*α cells to form *MAT***a**/α diploid cells. These diploid cells transcriptionally repress both copies of the mating loci, and therefore are no longer able to mate. Chromosome instability causes cells to randomly lose chromosomes during cell division. If a copy of chromosome III is lost, cells will regain the ability to mate. Diploid *his3*Δ*1* strains containing the various histone H3 mutations were patched and grown before replica plating to the lawn of *MAT***a** or *MAT*α tester strains (*lys1* and *thr3 met1*$^-$, respectively). Successful mating enabled the pseudotriploid to form colonies in minimal medium (Figure 5A). We quantified the number of colonies on the minimal medium plate and found that the wild-type and K14A strains displayed low levels of colony formation (Figure 5B), as expected from cells with normal chromosome stability. G44S mutant cells exhibited significantly higher rates of chromosome loss whereas the addition of K14A effectively reduced the number of colonies, suggesting that K14A also suppressed the chromosome instability defects caused by the G44S mutation.

A more quantitative approach to examining chromosome instability is by use of a synthetic chromosome bearing the *SUP11* tRNA suppressor for a chromogenic *ade2*$^-$ allele. Ade2p converts β-isopropylmalate to α-ketoisocaproate in leucine biosynthesis (Jones and Fink 1982). Accumulation of β-isopropylmalate gives *ade2*$^-$ colonies dark red coloration. Introducing the *SUP11* suppressor on a nonessential synthetic chromosome complements this defect and generates white colonies. Spontaneous loss of this synthetic chromosome causes the accumulation of the red pigmentation. Chromosome stability can thus be assessed by comparing the rate of colonies displaying significant red sectoring (Spencer *et al.* 1990). Specifically, we counted half-red/half-white colonies that resulted from a first-division chromosome loss event (Figure 6, arrows). Both wild-type and K14A strains

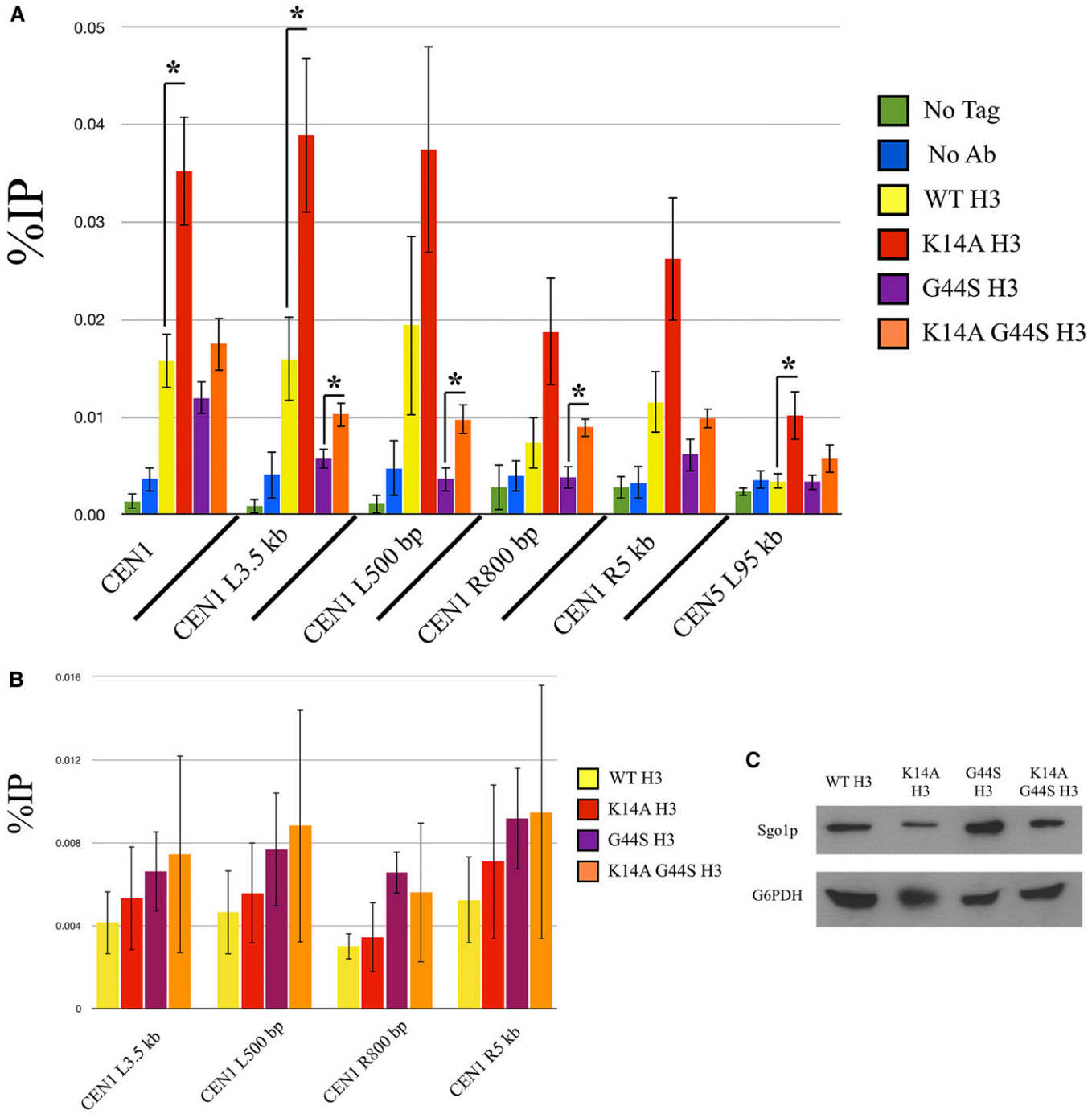

Figure 7 K14A enhances Sgo1p recruitment to chromatin in both WT and G44S strains. Strains with the indicated H3 backgrounds were synchronized with α factor, released into fresh medium, and grown for 60 min. Cells were then processed for either Sgo1p (A) or H3 (B) ChIP. ChIP DNA was analyzed using quantitative PCR and quantified as percent of IP. Four independent biological replicates were used to prepare this data. Error bars represent SD. * $P < 0.05$. (C) Western blot of Sgo1p expression levels as compared to G6PDH. (D) Sgo1p is eluted from chromatin at similar salt concentrations as histone H3 in all H3 backgrounds. (E) Cells with the indicated H3 backgrounds were synchronized in S phase by hydroxyurea treatment and released into fresh medium. DNA content was assessed by PI staining and flow cytometry. Ab, antibody; ChIP, chromatin immunoprecipitation; IP, immunoprecipitation; WT, wild-type.

had low rates of red sectoring, indicating high chromosome stability. As reported before, G44S cells had a high propensity of chromosome loss per 1000 cell divisions (Luo *et al.* 2010). On the other hand, K14A G44S cells were able to maintain the *SUP11* synthetic chromosome at a rate similar to that of wild-type cells. The number of half-red/half-white colonies was reduced significantly, indicating restoration of chromosome stability. From Figure 4, Figure 5, and Figure 6, we conclude that the K14A mutation effectively suppresses the mitotic defects caused by the G44S *tsm*$^{-}$ mutant allele.

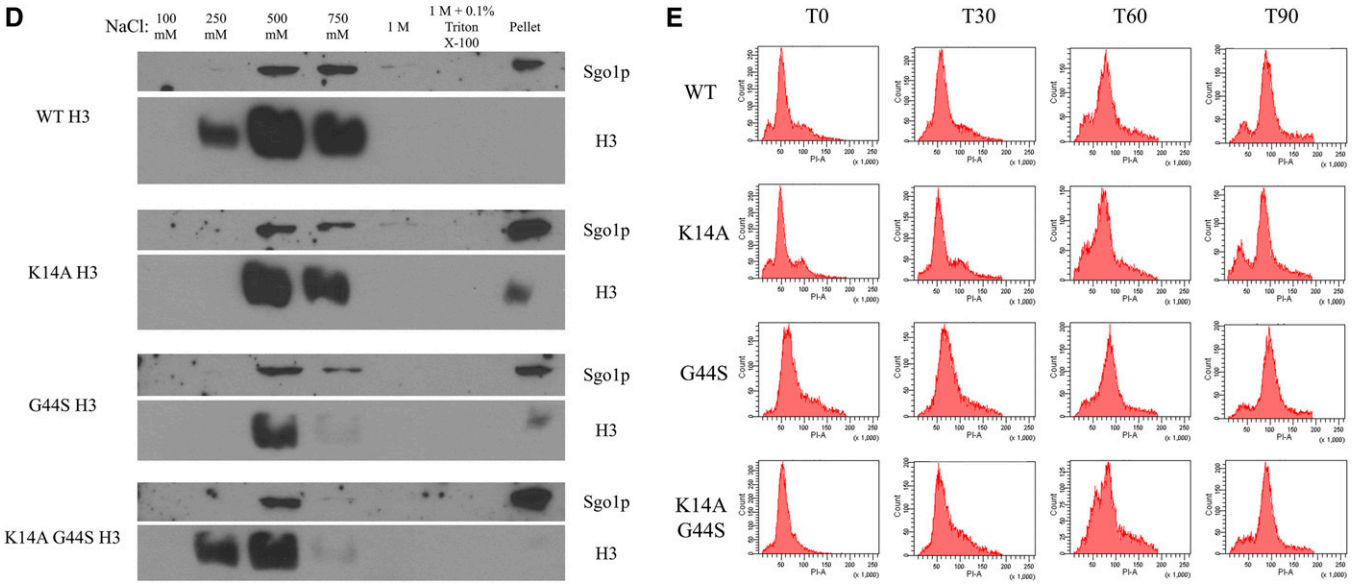

Figure 7 Continued.

K14A mutation increases pan-chromatin association of Sgo1p and binds Sgo1p physically. Previous work demonstrated that Sgo1p is recruited to both centromeres and pericentric regions during mitosis (Fernius and Hardwick 2007; Kiburz *et al.* 2008), and that the G44S mutation selectively affects the pericentric recruitment of Sgo1p (Luo *et al.* 2010). One possible explanation for the K14A-mediated suppression of *tsm*$^{-}$ defects is that Sgo1p regains its pericentric localization in this background. We conducted ChIP experiments with synchronized cultures to test this hypothesis (Figure 7A). Centromeric Sgo1p localization was normal in all H3 backgrounds, for H3 is replaced by Cse4p in centromeric nucleosomes (Meluh *et al.* 1998; Wieland *et al.* 2004). Sgo1p was also enriched at pericentromeres (yellow bars, Figure 7A), but is lost in G44S cells (purple bars). As predicted, the K14A G44S double mutant (orange bars) showed an apparent increase in pericentric Sgo1p abundance, consistent with the notion that retaining Sgo1p at the pericentric regions is a key determinant for the tension-sensing function of the SAC. However, K14A mutation achieves this suppression by allowing widespread association of Sgo1p with chromatin (red bars). All loci tested, proximal or distal to centromeres, showed significantly higher levels of Sgo1p, suggesting that K14 acetylation by Gcn5p has a global function that also includes the regulation of the SAC and tension sensing. This rescue was not due to a bulk increase in histone H3 recruitment to pericentric loci (Figure 7B), Sgo1p abundance alterations (Figure 7C), or deviations of the pace of cell cycle progression (Figure 7E). Furthermore, we examined the bulk association between Sgo1p and chromatin by stepwise salt washes of yeast nuclei. Figure 7D shows that Sgo1p was eluted from nuclear pellets by 500 mM or higher NaCl. This elution profile coincided with that of histone H3, indicating that the overall chromatin association of Sgo1p was not significantly affected by the three H3 alleles. Interestingly, in the two strains with the K14A mutation, Sgo1p appeared to be enriched in the final pellet fraction, after a high-salt and detergent wash, suggesting a new K14A allele-dependent tight target(s) for Sgo1p.

That K14A alone enables Sgo1p to appear in pericentric and arm regions of chromatin, even in the G44S background, suggests that the H3 tail may also be a target for Sgo1p binding. To test this notion, we fused GST to the tail domains of H3, Cse4p, and a kinetochore protein Cnn1p for pulldown assays. Cnn1p is associated with the outer kinetochore Ndc80 complex (Bock *et al.* 2012; Schleiffer *et al.* 2012, Thapa *et al.* 2015), and was therefore used as a negative control for Sgo1p interaction. Recombinant Sgo1p was tagged with SUMO to facilitate bacterial expression and solubility, and therefore SUMO was used as a negative control for the pulldown assays. Figure 8A shows that recombinant Sgo1p specifically interacts with the tail domains of H3 and Cse4p, but not that of Cnn1p or the GST control. This Sgo1p-Cse4p interaction is consistent with a recent report by Basrai and colleagues (Mishra *et al.* 2017). To test whether acetylation directly influences the H3 tail-Sgo1p interaction, we acetylated the H3 tail-GST fusion protein *in vitro* with Gcn5p (Figure 8B). To our surprise, acetylation did not cause an appreciable reduction of Sgo1p interaction *in vitro* (Figure 8C), suggesting the possibility of the existence of an additional factor(s) that acts downstream of Gcn5p-mediated H3 acetylation for more direct control of Sgo1p-chromatin association.

Discussion

We recently reported the identification and functional characterization of the TSM of H3 (^{42}KPGT), which is critical for faithful mitotic segregation (Luo *et al.* 2016). By retaining Sgo1p at the pericentric regions following its centromeric

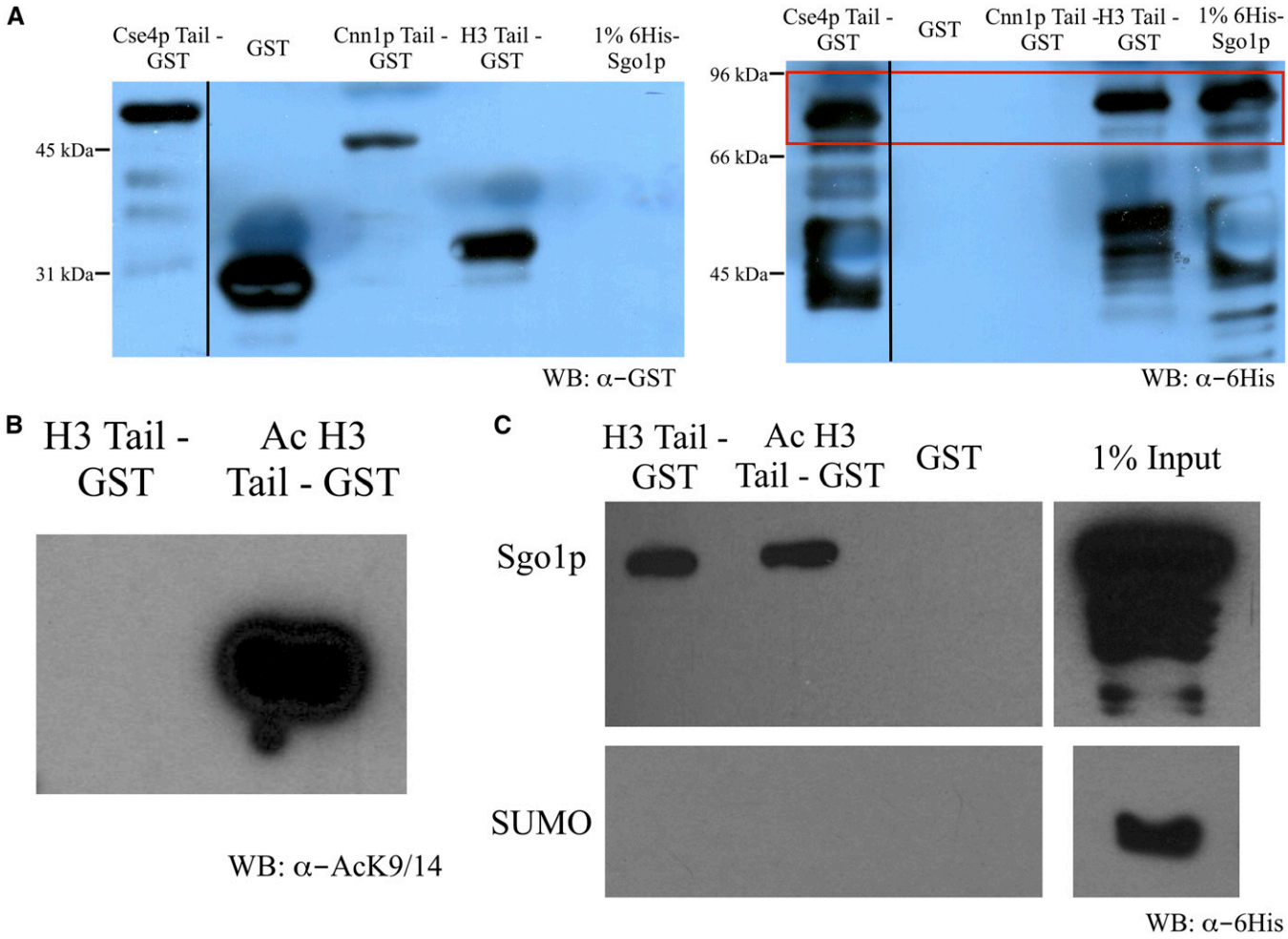

Figure 8 Sgo1p binds the histone H3 tail. (A) Tail peptides from Cse4p, Cnn1p, and histone H3 were C′-tagged with GST and bound to glutathione Sepharose beads. Beads were then mixed with 6His-Sgo1p and retained protein was assessed by immunoblotting. Full-length Sgo1p is displayed in the red box. (B) H3 tail peptide was either mock treated or *in vitro* acetylated by recombinant Gcn5p. Acetylation of histone H3 tail peptide at K9/14 was confirmed by immunoblotting with anti-acetylated K9/14 antibodies. (C) H3 tail peptides were mixed with a 6His-SUMO-Sgo1p or 6His-SUMO control and bound to glutathione Sepharose beads. Bound materials were analyzed by immunoblotting with anti-His tag antibodies. WB, western blot.

recruitment (Fernius and Hardwick 2007; Kawashima *et al.* 2010; Williams *et al.* 2017), the TSM ensures that cells establish bipolar attachment before initiating metaphase-to-anaphase transition. Here, we present evidence that Gcn5p likely exerts its TSM regulatory function by targeting selective lysine residues within the tail domain of histone H3. Significantly, pericentric localization of Sgo1p is partially restored in the H3 K14A G44S mutant, consistent with the notion that the presence of Sgo1p at pericentromeres is essential for the surveillance of mitotic tension between sister chromatids. While Sgo1p regains accessibility to pericentromeres in the K14A G44S background, the K14A mutation also renders it detectable in the arm region that is typically devoid of Sgo1p. Together with the biochemical evidence for the Sgo1p-H3 tail interaction, we suggest that the tail domain of H3 serves as an auxiliary anchor for Sgo1p. Under normal conditions, the TSM is the primary docking site for pericentric Sgo1p that is first recruited to the centromeres by phosphorylated H2A (Fernius and Hardwick 2007; Kawashima *et al.* 2010). Mutations at K42, G44, or T45 damage this binding surface and hence perturb the pericentric retention of Sgo1p spilled from centromeres. By deleting Gcn5p or mutating its major targets K14 or K23, the H3 tail assumes the capability of attracting Sgo1p to chromatin. The reappearance of the pericentric Sgo1p population thus restores the tension-sensing function. Genome-wide alteration of H3 acetylation status resulting from the loss of Gcn5p activity or tail K-to-A or -R mutations renders the arm region amenable to Sgo1p binding, therefore elevating Sgo1p abundance at these otherwise low-abundance areas of chromosomes.

It is also interesting that Sgo1p binds the H3 tail in a manner that does not seem to be affected appreciably by the acetylation status of the latter. This observation argues against the hypothesis that acetylation of the H3 tail by Gcn5p directly regulates Sgo1p binding, and instead suggests

the existence of additional regulators. For example, it is well documented that lysine acetylation attracts bromodomain-containing proteins for direct association (Dhalluin *et al.* 1999; Zhang *et al.* 2010; Gong *et al.* 2016). Acetylated K14 attracts yeast proteins such as Snf2p, Sth1p, and several Rsc proteins (Zhang *et al.* 2010). It is possible that one or more of these bromodomain proteins occlude Sgo1p from the tail domain. In the presence of a functional TSM, this occlusion does not impact SAC function, as Sgo1p binds the TSM at pericentric regions of chromatin. In *tsm*$^-$ strains, Sgo1p loses its pericentric footing, and therefore requires the interaction with the histone H3 tail to maintain a presence in pericentric chromatin. In this case, tail acetylation and competition from bromodomain proteins results in the loss of Sgo1p at the pericentric regions, and therefore impairs effective SAC function. Another possibility explaining the lack of effect on Sgo1p binding *in vitro* after acetylation is that an additional modification of the H3 tail *in vivo* (methylation or phosphorylation) potentiates the inhibitory activity of acetylated K14 on Sgo1p binding. Lastly, it is notable that the K14A mutation causes Sgo1p to spread to the arm regions of chromatin, raising an intriguing model that K14 acetylation limits Sgo1p to the pericentric region of chromatin.

This report shows a novel role of the histone H3 tail as a regulator in the maintenance of mitotic fidelity through the TSM. We also show that selective lysine residues in the H3 tail domain may facilitate Sgo1p function by helping the latter to maintain its pericentric footings. The critical, yet unanswered, question remains to be how Sgo1p relays the tension status to the activity of the SAC. It has been shown that the removal of Sgo1p from the pericentric region occurs after biorientation (Nerusheva *et al.* 2014). The tension-dependent conformational changes in the chromatin may be a determinant for Sgo1p-chromatin association (Haase *et al.* 2012; Verdaasdonk *et al.* 2012). We favor a scenario where tension-instigated conformational changes of chromatin are translated through the nucleosomes to deform the TSM of histone H3, which dislodges pericentric Sgo1p. After Sgo1p eviction from the pericentric regions of bioriented chromosome pairs, cells turn off the SAC and initiate the metaphase-to-anaphase transition. When the TSM is crippled, pericentric Sgo1p is retained by its association with the H3 tail in the absence of Gcn5p and other downstream effectors, such as one of the bromodomain-containing proteins. Spatially, the tail domain precedes the TSM. It seems plausible that the tension generated by biorientation may be transmissible from the TSM to the tail region (or vice versa). The restored pericentric Sgo1p population can then again monitor the tension status and relay that information to the SAC. This model also alludes to an intriguing hypothesis that the interplays between Gcn5p and the H3 tail may restrict Sgo1p from chromosomal arms. Further genetic and molecular dissection may shed light on the involvement of the H3 tail and its associated factors in the critical tension-sensing mechanism.

Literature Cited

Baker, S. P., J. Phillips, S. Anderson, Q. Qiu, J. Shabanowitz *et al.*, 2010 Histone H3 Thr 45 phosphorylation is a replication-associated post-translational modification in *S. cerevisiae*. Nat. Cell Biol. 12: 294–298.

Berger, S. L., 2007 The complex language of chromatin regulation during transcription. Nature 447: 407–412.

Blackwell, J. S., S. T. Wilkinson, N. Mosammaparast, and L. F. Pemberton, 2007 Mutational analysis of H3 and H4 N termini reveals distinct roles in nuclear import. J. Biol. Chem. 282: 20142–20150.

Bloom, K., S. Sharma, and N. V. Dokholyan, 2006 The path of DNA in the kinetochore. Curr. Biol. 16: 276–278.

Bock, L. J., C. Pagliuca, N. Kobayashi, R. A. Grove, Y. Oku *et al.*, 2012 Cnn1 inhibits the interactions between the KMN complexes of the yeast kinetochore. Nat. Cell Biol. 14: 614–624.

Dai, J., E. M. Hyland, D. S. Yuan, H. Huang, J. S. Bader *et al.*, 2008 Probing nucleosome function: a highly versatile library of synthetic histone H3 and H4 mutants. Cell 134: 1066–1078.

Dhalluin, C., J. E. Carlson, L. Zeng, C. He, A. K. Aggarwal *et al.*, 1999 Structure and ligand of a histone acetyltransferase bromodomain. Nature 399: 491–496.

Fernius, J., and K. G. Hardwick, 2007 Bub1 kinase targets Sgo1 to ensure efficient chromosome biorientation in budding yeast mitosis. PLoS Genet. 3: 2312–2325.

Gietz, D., A. St. John, R. A. Woods, and R. H. Schiestl, 1992 Improved method for high efficiency transformation of intact yeast cells. Nucleic Acids Res. 20: 1425.

Glotzer, M., 1996 Mitosis: don't get mad, get even. Curr. Biol. 6: 1592–1594.

Gong, F., L.-Y. Chiu, and K. M. Miller, 2016 Acetylation reader proteins: linking acetylation signaling to genome maintenance and cancer. PLoS Genet. 12: e1006272.

Haase, J., A. Stephens, J. Verdaasdonk, E. Yeh, and K. Bloom, 2012 Bub1 kinase and Sgo1 modulate pericentric chromatin in response to altered microtubule dynamics. Curr. Biol. 22: 471–481.

Hunt, C. R., D. Ramnarain, N. Horikoshi, P. Iyengar, R. K. Pandita *et al.*, 2013 Histone modifications and DNA double-strand break repair after exposure to ionizing radiations. Radiat. Res. 179: 383–392.

Indjeian, V. B., B. M. Stern, and A. W. Murray, 2005 The centromeric protein Sgo1 is required to sense lack of tension on mitotic chromosomes. Science 307: 130–133.

Jeganathan, K., L. Malureanu, D. J. Baker, S. C. Abraham, and J. M. van Deursen, 2007 Bub1 mediates cell death in response to chromosome missegregation and acts to suppress spontaneous tumorigenesis. J. Cell Biol. 179: 255–267.

Jones, E. W., and G. R. Fink, 1982 Regulation of amino acid and nucleotide biosynthesis in yeast, pp. 181–299 in *Molecular Biology of the Yeast Saccharomyces: Metabolism and Gene Expression*. Cold Spring Harbor Press, Cold Spring Harbor, NY.

Kasten, M., H. Szerlong, H. Erdjument-Bromage, P. Tempst, M. Serner *et al.*, 2004 Tandem bromodomains in the chromatin remodeler RSC recognize acetylated histone H3 Lys14. EMBO 23: 1348–1359.

Kawashima, S., Y. Nukabayashi, K. Matsubara, N. Sano, T. Enomoto *et al.*, 2011 Global analysis of core histones reveals nucleosomal surfaces required for chromosome bi-orientation. EMBO 30: 3353–3367.

Kawashima, S. A., Y. Yamagishi, T. Honda, K.-I. Ishiguro, and Y. Watanabe, 2010 Phosphorylation of H2A by Bub1 prevents chromosomal instability through localization shugoshin. Science 327: 172–177.

Kiburz, B. M., A. Amon, and A. L. Marston, 2008 Shugoshin promotes sister kinetochore biorientation in Saccharomyces cerevisiae. Mol. Biol. Cell 19: 1199–1209.

Kitajima, T. S., S. Hauf, M. Ohsugi, T. Yamamoto, and Y. Watanabe, 2005 Human Bub1 defines the persistent cohesion site along the mitotic chromosome by affecting shugoshin localization. Curr. Biol. 15: 353–359.

Kitajima, T. S., T. Sakuno, K.-I. Ishiguro, S.-I. Iemura, T. Natsume *et al.*, 2006 Shugoshin collaborates with protein phosphatase 2A to protect cohesin. Nature 441: 46–52.

Koc, A., L. J. Wheeler, C. K. Mathews, and G. F. Merrill, 2004 Hydroxyurea arrests DNA replication by a mechanism that preserves basal dNTP pools. J. Biol. Chem. 279: 223–230.

Kuo, M.-H., J. E. Brownell, R. E. Sobel, T. A. Ranalli, R. G. Cook *et al.*, 1996 Transcription-liked acetylation by Gcn5p of histones H3 and H4 at specific lysines. Nature 383: 269–272.

Kuo, M.-H., J. Zhou, P. Jambeck, M. E. Churchill, and C. D. Allis, 1998 Histone acetyltransferase activity of yeast Gcn5p is required for the activation of target genes in vivo. Genes Dev. 12: 627–639.

Kuo, Y.-M., and A. J. Andrews, 2012 Quantitating the specificity and selectivity of Gcn5-mediated acetylation of histone H3. PLoS One 8: e54896.

Lew, D. J., and D. J. Burke, 2003 The spindle assembly and spindle position checkpoints. Annu. Rev. Genet. 37: 251–282.

Liu, Y., X. Xu, S. Singh-Rodriguez, Y. Zhao, and M.-H. Kuo, 2005 Histone H3 Ser10 phosphorylation-independent function of Snf1 and Reg1 proteins rescues a *gcn5*$^{-}$ mutant in *HIS3* expression. Mol. Cell. Biol. 25: 10566–10579.

Loncarek, J., O. Kisurina-Evgenieva, T. Vinogradova, P. Hergert, S. La Terra *et al.*, 2007 The centromere geometry essential for keeping mitosis error free is controlled by spindle forces. Nature 450: 745–749.

Luger, K., A. W. Mäder, R. K. Richmond, D. F. Sargent, and T. J. Richmond, 1997 Crystal structure of the nucleosome core particle at 2.8 A resolution. Nature 389: 251–260.

Luo, J., X. Xu, H. Hall, E. M. Hyland, J. D. Boeke *et al.*, 2010 Histone H3 exerts a key function in mitotic checkpoint control. Mol. Cell. Biol. 30: 537–549.

Luo, J., X. Deng, C. Buehl, X. Xu, and M.-H. Kuo, 2016 Identification of tension sensing motif of histone H3 in *Saccharomyces cerevisiae* and its regulation by histone modifying enzymes. Genetics 204: 1029–1043.

Megee, P. C., B. A. Morgan, and M. M. Smith, 1995 Histone H4 and the maintenance of genome integrity. Genes Dev. 9: 1716–1727.

Meluh, P. B., P. Yang, L. Glowczewski, D. Koshland, and M. M. Smith, 1998 Cse4p is a component of the core centromere of Saccharomyces cerevisiae. Cell 94: 607–613.

Mishra, P. K., K. Thapa, P. Chen, S. Wang, T. R. Hazbun, and M. A. Basrai, 2017 Budding yeast CENP-ACse4 interacts with the N-terminus of Sgo1 and regulates its association with centromeric chromatin. Cell Cycle October 5, 2017.

Nerusheva, O. O., S. Galander, J. Fernius, D. Kelly, and A. L. Marston, 2014 Tension-dependent removal of pericentromeric shugoshin is an indicator of sister chromosome biorientation. Genes Dev. 28: 1291–1309.

Ng, T. M., T. L. Lenstra, N. Duggan, S. Jiang, S. Ceto *et al.*, 2013 Kinetochore function and chromosome segregation rely on critical residues in histones H3 and H4 in budding yeast. Genetics 195: 795–807.

Pinsky, B. A., and S. Biggins, 2005 The spindle checkpoint: tension *vs.* attachment. Trends Cell Biol. 15: 486–493.

Ramachandran, S., and S. Henikoff, 2015 Replicating nucleosomes. Sci. Adv. 1: e1500587.

Santaguida, S., and A. Amon, 2015 Short- and long-term effects of chromosome mis-segregation and aneuploidy. Nat. Rev. Mol. Cell Biol. 16: 473–485.

Schleiffer, A., M. Maier, G. Litos, F. Lampert, P. Hornung *et al.*, 2012 CENP-T proteins are conserved centromere receptors of the Ndc80 complex. Nat. Cell Biol. 14: 604–613.

Sherman, F., 1991 Getting started with yeast. Methods Enzymol. 194: 3–21.

Slater, M. L., 1973 Effect of reversible inhibition of deoxyribonucleic acid synthesis on the yeast cell cycle. J. Bacteriol. 113: 263–270.

Spencer, F., S. L. Gerring, C. Connelly, and P. Hieter, 1990 Mitotic chromosome transmission fidelity mutants in *Saccharomyces cerevisiae*. Genetics 124: 237–249.

Thapa, K. S., A. Oldani, C. Pagliuca, P. De Wulf, and T. R. Hazbun, 2015 The Mps1 kinase modulates the recruitment and activity of Cnn1 CENP-T at Saccharomyces cerevisiae kinetochores. Genetics 200: 79–90.

Verdaasdonk, J. S., R. Gardner, A. D. Stephens, E. Yeh, and K. Bloom, 2012 Tension-dependent nucleosome remodeling at the pericentromere in yeast. Mol. Biol. Cell 23: 2560–2570.

Vernarecci, S., P. Ornaghi, A. Bagu, E. Cundari, P. Ballario, and P. Filetici, 2008 Gcn5p Plays an Important Role in Centromere Kinetochore Function in Budding Yeast. Mol. Cell. Biol. 28(3): 988–96.

Wang, X., and W. Dai, 2005 Shugoshin, a guardian for sister chromatid segregation. Exp. Cell Res. 310: 1–9.

Wieland, G., S. Orthaus, S. Ohndorf, S. Diekmann, and P. Hemmerich, 2004 Functional complementation of human centromere protein A (CENP-A) by Cse4p from Saccharomyces cerevisiae. Mol. Cell. Biol. 24: 6620–6630.

Williams, S. J., A. Abrieu, and A. Losada, 2017 Bub1 targeting to centromeres is sufficient for Sgo1 recruitment in the absence of kinetochores. Chromosoma 126: 279–286.

Yamagishi, Y., T. Sakuno, M. Shimura, and Y. Watanabe, 2008 Heterochromatin links to centromeric protection by recruiting shugoshin. Nature 455: 251–255.

Yamagishi, Y., T. Honda, Y. Tanno, and Y. Watanabe, 2010 Two histone marks establish the inner centromere and chromosome bi-orientation. Science 330: 239–243.

Zhang, Q., S. Chakravarty, D. Ghersi, L. Zeng, A. N. Plotnikov *et al.*, 2010 Biochemical profiling of histone binding selectivity of the yeast bromodomain family. PLoS One 5: e8903.

Zhang, W., J. R. Bone, D. G. Edmondson, B. M. Turner, and S. Y. Roth, 1998 Essential and redundant functions of histone acetylation revealed by mutation of target lysine and loss of the Gcn5p acetyltransferase. EMBO J. 17: 3155–3167.

Communicating editor: S. Sharan